https://doi.org/10.5194/egusphere-2026-830
Preprint. Discussion started: 28 April 2026

Seasonal dynamics of eutrophication in human-impacted rivers

Alexander Hubig[1], Pia Ebeling[1], Daniel Graeber[2], Ulrike Scharfenberger[2], and Andreas Musolff[1]
[1]Department of Hydrogeology, Helmholtz-Centre for Environmental Research - UFZ, Leipzig, Germany
[2]Department of Aquatic Ecosystem Analysis, Helmholtz-Centre for Environmental Research - UFZ, Magedeburg, Germany
Correspondence: Alexander Hubig (alexander.hubig@ufz.de)

Abstract. Eutrophication - i.e., biomass overproduction due to nutrient enrichment - persists as a threat to riverine ecosystems despite achievements in lowering phosphorus (P) concentrations. This study explores seasonal patterns and drivers of chlorophyll a (Chl-a) linked with P availability across a selection of human-impacted rivers in Germany. We analyzed Chl-a and total phosphorus (TP) concentration measurements from 133 river sites and quantified their relationship using the degree of realized eutrophication ($\alpha_{realized}$) – the ratio of measured to maximum Chl-a at a given TP. By applying k-means clustering on seasonal $\alpha_{realized}$ cycles, we identified five archetypal patterns. To understand the drivers of these patterns, we examined the seasonal dynamics of total nitrogen (TN), the TN:TP ratio, and fractions of reactive P and N. We further conducted a correlation analysis of $\alpha_{realized}$ and photosynthetically active radiation (PAR), water temperature, and discharge. In addition, we compared static river network and catchment characteristics between the clusters. We found that (1) constantly high $\alpha_{realized}$ was associated with close upstream lakes, along with nutrient concentrations suggesting co-control of Chl-a by P and N. (2) High $\alpha_{realized}$ in mostly lake-free rivers throughout spring and summer were associated with light control, as indicated by a high correlation with PAR. (3) Rivers with spring peaks and low summer $\alpha_{realized}$ were explained by summer Chl-a losses through grazing. Here, differences in spring peak timing and intensity could be related to differences in land use, hinting to riparian shading as a modulator of phytoplankton growth. Therefore, we find especially high risk of phytoplankton blooms downstream of lakes throughout the vegetation period, in long rivers without effective grazer control from mid-spring to early autumn, and in rivers with a lack of riparian shading during spring. Effective management may comprise dual management of P and N, especially for locations prone to summer blooms, and targeted riparian shading as an additional measure.

1 Introduction

Overproduction of biomass due to anthropogenically increased nutrient levels, known as eutrophication, is a widespread threat to both marine and freshwater ecosystems (e.g., Le Moal et al., 2019; Wurtsbaugh et al., 2019). The elevated nutrient levels in water bodies, particularly phosphorus (P) and nitrogen (N), originate from wastewater inputs, agriculture, and industrial activities (e.g., Le Moal et al., 2019). The consequences of eutrophication in coastal systems include extensive dead zones caused by severe oxygen depletion, which threaten biodiversity and fisheries (e.g., Davidson et al., 2014; Wurtsbaugh et al., 2019). In freshwater systems, eutrophication, especially when associated with harmful algal blooms, can cause widespread die-offs of aquatic organisms and affect clean water supplies for human use (e.g., Le Moal et al., 2019; Wurtsbaugh et al., 2019; de Vries et al., 2024; Wang et al., 2024).

https://doi.org/10.5194/egusphere-2026-830
Preprint. Discussion started: 28 April 2026

In the 1970s and 1980s, reduced P inputs from wastewater point sources lowered phytoplankton levels in freshwater ecosystems in many countries worldwide (e.g., Friedrich and Pohlmann, 2009; Minaudo et al., 2015; Le Moal et al., 2019; Westphal et al., 2019, 2020). However, despite these reduction efforts, phytoplankton overproduction with its adverse effects persists, partly linked to changing hydroclimatic conditions (e.g., Bowes et al., 2012b; Wurtsbaugh et al., 2019; Kleinteich et al., 2024). Climate change, along with associated heat waves and droughts, is likely to further increase the frequency of phytoplankton blooms (Whitehead et al., 2009; Kamjunke et al., 2021; Kleinteich et al., 2024) and to provide a competitive advantage to harmful cyanobacteria (Paerl and Huisman, 2008; Wagner and Adrian, 2009; Kleinteich et al., 2024). Managing the threat of future increases in phytoplankton concentrations requires a comprehensive understanding of where and when excessive phytoplankton growth may occur in complex, coupled human-natural freshwater systems.

While both lakes and rivers face the challenge of eutrophication, rivers have been less studied than lakes (Wurtsbaugh et al., 2019). Rivers differ from lakes in the spatial and temporal characteristics of water residence time, light availability, and the composition and functioning of their plankton communities (Reynolds et al., 1994). At the same time, eutrophication processes in upstream lakes can significantly influence downstream river eutrophication (Hubig et al., 2025). Spatial patterns of chlorophyll a (Chl-a) concentrations in rivers, which represent phytoplankton biomass, have been studied individually (e.g., Søballe and Kimmel, 1987; Neal et al., 2006) and in relation to total phosphorus (TP) to separate the effects of elevated P concentrations from other controlling factors (Mischke et al., 2011; Bowes et al., 2012a; Hubig et al., 2025). A key finding of these studies is that water residence time is a major control of the incorporation of available P by growing phytoplankton. Therefore, efficient uptake of P into biomass and high Chl-a concentrations are typically found in long rivers (Søballe and Kimmel, 1987; Neal et al., 2006; Mischke et al., 2011; Istvánovics and Honti, 2012; Hubig et al., 2025), rivers with upstream lakes (Søballe and Kimmel, 1987; Hubig et al., 2025), or rivers with anthropogenic modifications such as reservoirs, dams, or canals (Søballe and Kimmel, 1987; Bowes et al., 2012a).

While we have developed substantial knowledge on the controls of the spatial Chl-a patterns in river networks and their linkage to P availability, their temporal variability is insufficiently understood: By relying on temporal averages, static river network properties, and catchment characteristics, the above-mentioned studies do not provide insights into the variability that phytoplankton biomass may exhibit on seasonal or inter-annual scales. This poses the risk of missing events with exceedance of critical Chl-a levels causing the eutrophication impacts described above. Understanding the magnitude and timing of these exceedance events and their underlying drivers is crucial for managing water quality in river networks.

Elevated Chl-a levels in rivers are typically reported in spring, often followed by a period of low Chl-a in summer (e.g., Gosselain et al., 1998; Skidmore et al., 1998; Balbi, 2000). However, separate summer peaks and occasional autumn peaks also occur, often associated with different phytoplankton species (e.g., Ha et al., 1998; Ibelings et al., 1998; Neal et al., 2006; Friedrich and Pohlmann, 2009; Minaudo et al., 2015; Kleinteich et al., 2024). While spring peaks are usually composed of diatoms, they are often succeeded by other phytoplankton groups such as green algae or cyanobacteria later in the year (Garnier et al., 1995; Friedrich and Pohlmann, 2009; Kleinteich et al., 2024). In lakes, such plankton successions are described by the well-established plankton ecology group (PEG) model (Sommer et al., 1986, 2012). Because many rivers are affected by upstream lakes in terms of eutrophication (e.g., Köhler, 1994; Hubig et al., 2025), their seasonal patterns may more closely

https://doi.org/10.5194/egusphere-2026-830
Preprint. Discussion started: 28 April 2026

follow the PEG model than those of rivers without lake impacts. Overall, the seasonal patterns of Chl-a can vary greatly across locations and also years at the same site due to different controlling factors.

Concentrations of the highly phytoplankton-growth relevant nutrients P and N often show opposing seasonal patterns in anthropogenically impacted areas. In Germany, P from wastewater point sources has its maximum mostly during low-flow conditions in summer, while N, mostly emerging from diffuse agricultural inputs, has its maximum typically during high-flow conditions in winter (Westphal et al., 2020; Ebeling et al., 2021; Wachholz et al., 2022, 2024; Ebeling et al., 2026). This implies not only a variable absolute availability of nutrients for phytoplankton growth, but also seasonal changes in the N:P stoichiometry, resulting in potential shifts between N and P control of phytoplankton during the year. While potential N and P co-limitation of riverine phytoplankton growth has also been discussed in recent years (e.g., Dodds and Smith, 2016; Wurtsbaugh et al., 2019), co-limitation of lake phytoplankton by both N and P instead of P alone seems to be the case for a majority of lakes, as recent large-scale studies (Moon et al., 2021; Graeber et al., 2024) and whole ecosystem experimental studies (Andersen et al., 2025) show. Hence, N and P co-limitation may be particularly important for rivers heavily impacted by upstream lakes (Hubig et al., 2025).

Light availability in streams and rivers, which is crucial for phytoplankton growth, is primarily driven by the seasonal variation of sunlight and modulated to a large degree by riparian shading (Julian et al., 2008; Hutchins et al., 2010; Bowes et al., 2012b) and discharge (Julian et al., 2008; Hardenbicker et al., 2014; Kamjunke et al., 2021). As a consequence, phytoplankton blooms may be more common and intense in areas with riparian clearcutting, such as agricultural lands (Mosisch et al., 2001; Bowes et al., 2012b; Rode et al., 2016), and under low-flow conditions, when water depth is shallower, turbidity is lower, and hence there is a higher light availability throughout the water column (Julian et al., 2008; Kamjunke et al., 2021). Low-flow conditions are also associated with higher residence times, which further support phytoplankton growth (Reynolds, 2000). These characteristics of low-flow situations may influence the seasonal patterns of eutrophication by shaping spring blooms, which can be triggered by decreasing discharge in spring (Garnier et al., 1995; Hardenbicker et al., 2014), and by causing summer blooms during periods of low summer discharge (Kamjunke et al., 2021).

Water temperature is an additional factor controlling the seasonal patterns of river eutrophication (e.g., Desortová and Punčochář, 2011; Bowes et al., 2016). Its influence, however, is complex, as it affects phytoplankton growth as well as grazing activities. Phytoplankton growth rates increase with water temperature, but decrease when water temperature exceeds a tolerable maximum. Thereby, growth rate functions are highly species-dependent, making water temperature decisive for competition between different phytoplankton groups (e.g., Garnier et al., 1995; Paerl and Otten, 2013). Phytoplankton loss commonly occurs due to zooplankton grazing (Gosselain et al., 1998), while benthic filter feeders, such as mussels, also can substantially reduce phytoplankton densities in rivers (Welker and Walz, 1998; Weitere and Arndt, 2002; Graeber et al., 2013; Pigneur et al., 2014; Hardenbicker et al., 2016). For benthic filter feeders, positive relationships between water temperature and filtration rates have been found (Lei et al., 1996; Weitere and Arndt, 2002; Pigneur et al., 2014), leading to the highest loss rates in summer (Pigneur et al., 2014).

Despite the recognition of these various controlling factors, large-scale studies quantifying their importance in driving seasonal patterns of riverine phytoplankton across locations in a human-impacted landscape remain scarce. Here, we investigate

https://doi.org/10.5194/egusphere-2026-830
Preprint. Discussion started: 28 April 2026

the seasonal variability of eutrophication across sites utilizing a Germany-wide water quality dataset previously introduced by Hubig et al. (2025). We specifically focus on the degree of realized eutrophication $\alpha_{realized}$, a measure developed to quantify the sensitivity of riverine phytoplankton biomass to P availability (Hubig et al., 2025). Unlike Chl-a concentration, $\alpha_{realized}$ also distinguishes rivers where P is abundant but phytoplankton cannot fully exploit it due to other growth-limiting factors or biomass loss processes. By that, $\alpha_{realized}$ provides a new view on freshwater eutrophication and its management beyond the assessment of Chl-a concentration. Hubig et al. (2025) found that particularly long rivers and short rivers with lakes in the upstream network reach a high median annual $\alpha_{realized}$, implying that P uptake by phytoplankton is more efficient there and that phytoplankton growth dominates over loss. Here, we analyze the seasonal patterns of $\alpha_{realized}$ of 133 stations with good seasonal coverage to investigate at which times of the year P is used efficiently by phytoplankton and at which times loss processes reduce this efficiency. Applying a k-means clustering algorithm to the $\alpha_{realized}$ time series, we (1) identify stations with similar, archetypal seasonal dynamics of $\alpha_{realized}$. To determine, which factors explain the observed dynamics, we (2) analyze the seasonal patterns of concentrations and the stoichiometry of nutrients as well as of potential physical drivers of $\alpha_{realized}$ for each cluster. By (3) further examining static river network properties and catchment characteristics, we discuss through which processes they may modulate the temporal drivers of $\alpha_{realized}$. Finally, we (4) identify critical times and locations for elevated phytoplankton concentrations and discuss implications for the operational space of river management.

2 Material and Methods

2.1 Data base compilation and processing

2.1.1 Time series data

In this study, we used a comprehensive observational dataset of chlorophyll a (Chl-a), total phosphorus (TP), soluble reactive phosphorus (SRP), total nitrogen (TN), dissolved inorganic nitrogen (DIN, as the sum of NO_3-N, NO_2-N, and NH_4-N), water temperature (T_{water}), discharge (Q), and photosynthetically active radiation (PAR) from river locations across Germany. Except PAR, data are in large part included in the QUADICA database (Ebeling et al., 2022, 2026), with additional data provided by German authorities. The dataset was described in detail by Hubig et al. (2025) and comprises 329 stations (Figure 1) covering 31,661 samples for which at least Chl-a and TP measurements were available. Data consist of grab samples taken between 2000 and 2019, with measurements from the winter months (December, January, February) excluded. Following Hubig et al. (2025), Chl-a, TP, SRP, TN, NO_3-N, NO_2-N, and NH_4-N concentration measurements below the limit of quantification were imputed for each station by regression on order statistics. PAR was derived analogously to Hubig et al. (2025) from surface shortwave downwelling radiation obtained from the Copernicus E-OBS data product (Copernicus Climate Change Service, 2020; Cornes et al., 2018). Surface shortwave downwelling radiation was converted to PAR according to Scharfenberger et al. (2019).

https://doi.org/10.5194/egusphere-2026-830
Preprint. Discussion started: 28 April 2026

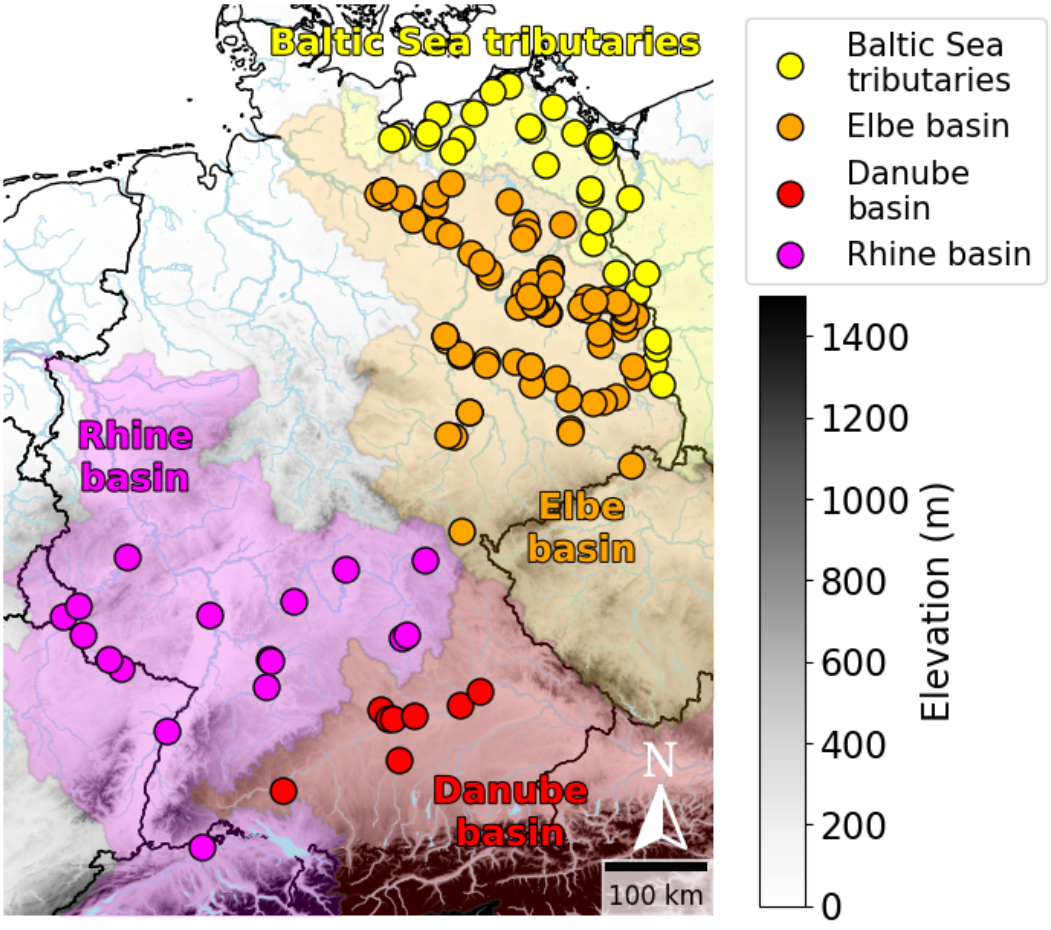

Figure 1. Location of the 133 stations of the water quality dataset of this study in Germany.

2.1.2 Data selection and study sites

To ensure sufficient coverage of the entire growing season at all stations, we applied strict selection criteria to the time-series data, resulting in the exclusion of some years of measurements and some stations from the original dataset (Hubig et al., 2025). The criteria for including measurement years were as follows: (1) The first measurement day of a year at a given station must not be later than March 18 (median first day of measurements across all data). (2) The last measurement day of a year at a given station must not be earlier than November 6 (median last day of measurements across all data). (3) The number of measurements must be at least 9 for each year (median number of measurements per year across the original stations). After excluding station-specific years that did not meet these criteria, we further omitted all stations with fewer than three remaining years. As a result, the final dataset comprised 133 stations and 898 years with 12,292 individual measurement days with concurrent Chl-a and TP data (Figure 1, Table 1). Out of these stations, SRP is available at 130 stations (883 years, 11,995

https://doi.org/10.5194/egusphere-2026-830
Preprint. Discussion started: 28 April 2026

Table 1. Overview of the parameters of this study.

Parameter Long name	Parameter Short name	Unit	Measurements	Covered annual cycles	Stations
Original dynamic parameters					
Chlorophyll a	Chl-a	µg/l	12,292	898	133
Total phosphorus	TP	mg/l	12,292	898	133
Total nitrogen	TN	mg/l	7,106	529	70
Soluble reactive phosphorus	SRP	mg/l	11,995	883	130
Dissolved inorganic nitrogen	DIN	mg/l	10,440	801	120
Water temperature	T_{water}	°C	12,237	895	132
Photosynthetically active radiation	PAR	µmol/m^2/s	11,777	857	127
Discharge	Q	m^3/s	5,950	415	54
Calculated dynamic parameters					
Degree of realized eutrophication	$\alpha_{realized}$	%	12,292	898	133
TN:TP ratio	TN:TP	mol/mol	7,106	529	70
Reactive N fraction	DIN:TN	mol/mol	6,584	501	66
Reactive P fraction	SRP:TP	mol/mol	10,440	801	120
Static parameters					
River length	L_{river}	km	-	-	133
Distance to nearest lake	d_{lake}	km	-	-	119
Lake residence time density	τ_{lakes}	days/km	-	-	132
Agricultural land cover	f_{agric}	%	-	-	58
Forested land cover	f_{forest}	%	-	-	58
Population density	$pdens$	inhab./km^2	-	-	58

measurements), TN at 70 stations (529 years, 7,106 measurements), DIN at 120 stations (801 years, 10,440 measurements), T_{water} at 132 stations (895 years, 12,237 measurements), PAR at 127 stations (857 years, 11,777 measurements), and Q at 54 stations (415 years, 5,950 measurements, all in Table 1). For all parameters, only measurement days with coinciding Chl-a and TP measurements were included.

More than half of the stations (78) are located in the Elbe basin in northeastern Germany, which extends over large parts of the North German Lowland (Figure 1). The remaining stations are distributed across several Baltic Sea tributaries (30 stations, also in the North German Lowland), as well as the Danube (8 stations) and Rhine basins (17 stations) in the more mountainous southern Germany (Figure 1). As in Hubig et al. (2025), we excluded the Weser and Ems basins, along with smaller North Sea catchments, due to limited data availability in northwestern Germany.

https://doi.org/10.5194/egusphere-2026-830
Preprint. Discussion started: 28 April 2026

2.1.3 River network properties and catchment characteristics

River network properties were quantified as river length (L_{river}), distance to the nearest upstream lake (d_{lake}), and lake residence time density (τ_{lakes}) according to Hubig et al. (2025). In short, based on the HydroRIVERS river network (Lehner and Grill, 2013), L_{river} was defined as the longest path from the measurement station in the upstream river network. For each station, d_{lake} was determined as the shortest distance along the network to a lake polygon intersecting with the upstream network (lake polygons taken from the HydroLAKES database, Messager et al., 2016). Water residence times of all lake polygons intersecting with the respective upstream networks were summed and divided by the network length to obtain τ_{lakes}. Only lake polygons with a residence time of at least one full day were included. We note that for 14 stations, no lake polygon was intersecting with the upstream network so that d_{lake} could not be obtained (Table 1). Analogously, one station was located within a lake polygon (d_{lake} = 0 km) so that τ_{lakes} could not be obtained.

The catchment characteristics agricultural land cover fraction (f_{agric}), forested land cover fraction (f_{forest}), and population density ($pdens$) were obtained from the QUADICA dataset (Ebeling et al., 2022, 2026). Of the 133 stations of our study, 58 are part of QUADICA and could be linked with the catchment characteristics listed above (Table 1).

2.2 Data analysis

2.2.1 Metrics to assess eutrophication

For each measurement pair, we used the Chl-a and TP measurements to calculate the degree of realized eutrophication ($\alpha_{realized}$), introduced by Hubig et al. (2025) as:

$$\alpha_{realized} = \frac{\text{Chl-}a}{\text{Chl-}a_{potential}} \cdot 100\%. \tag{1}$$

The purpose of $\alpha_{realized}$ is to quantify the realized, i.e., the measured Chl-a relative to a theoretical upper limit (Chl-$a_{potential}$) at a given TP level (Figure 2). Chl-$a_{potential}$ is calculated as:

$$\text{Chl-}a_{potential} = \frac{\theta_{\text{Chl-}a}}{\theta_{\text{P},min}} \cdot \text{TP}, \tag{2}$$

where $\theta_{\text{Chl-}a}$ is the Chl-a content of phytoplankton expressed on a cellular carbon basis (g Chl-a g C^{-1}) and $\theta_{\text{P},min}$ is the minimum P content of phytoplankton cells (g P g C^{-1}). As described in Hubig et al. (2025), the species-specific $\theta_{\text{P},min} = 0.00552$ g P g C^{-1} was calculated as the median of a dataset of phytoplankton species compiled from literature (Schwaderer et al., 2011; Edwards et al., 2013, 2015). We further assumed $\theta_{\text{Chl-}a}$ = 0.03 g Chl-a g C^{-1} (Riemann et al., 1989). The resulting equation is:

$$\alpha_{realized} = \frac{\theta_{\text{P},min}}{\theta_{\text{Chl-}a}} \cdot \frac{\text{Chl-}a}{\text{TP}}, \tag{3}$$

where $\alpha_{realized}$ is proportional to the ratio of measured Chl-a and TP. Most analyses in this study focus on $\alpha_{realized}$. When addressing Chl-a alone, we use a Chl-a concentration threshold of 30 µg/l, taken from Dodds et al. (1998), to define phytoplankton blooms (Figure 2).

https://doi.org/10.5194/egusphere-2026-830
Preprint. Discussion started: 28 April 2026

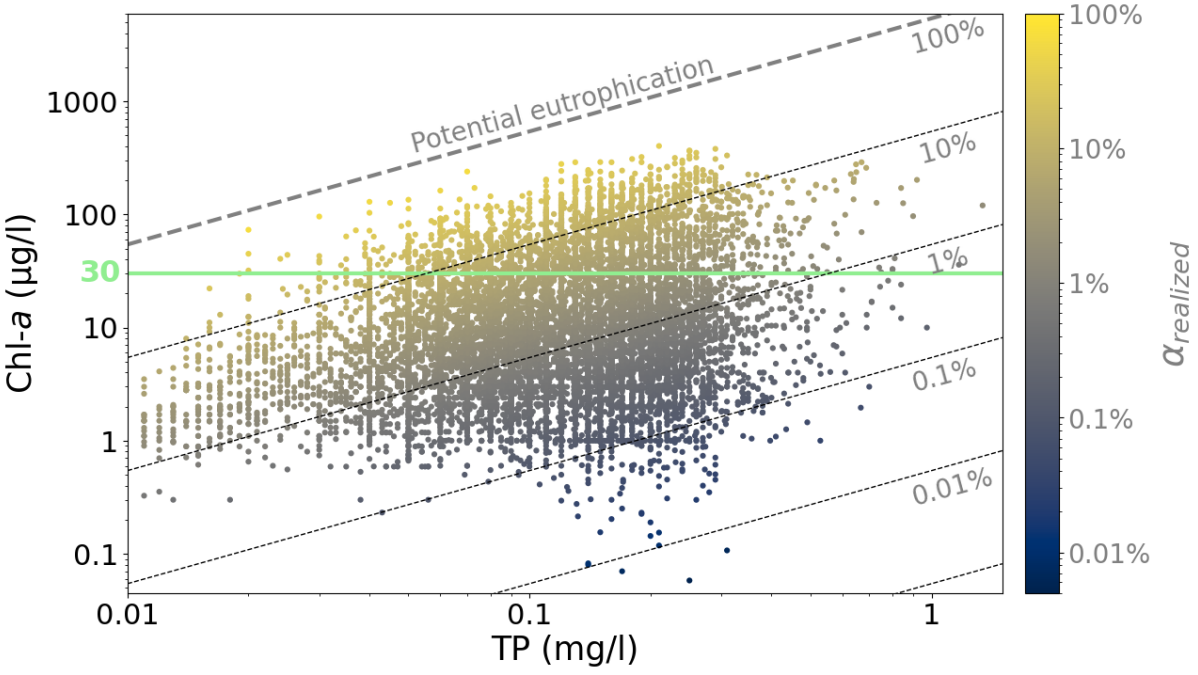

Figure 2. Scatter plot of all measured TP and Chl-a concentrations that were included in the analysis of seasonal archetypes. The green line marks the Chl-a concentration threshold for phytoplankton blooms (Dodds et al., 1998). For each pair of TP and Chl-a concentrations, the degree of realized eutrophication, $\alpha_{realized}$, is shown by colors and dashed lines.

In addition to $\alpha_{realized}$, we calculated molar TN:TP ratios to assess stations for potential N and P co-deficiency. We used the thresholds TN:TP = 20 for N deficiency and TN:TP = 50 for P deficiency established in lakes (Guildford and Hecky, 2000; Graeber et al., 2024). Finally, we calculated the reactive nutrient fractions DIN:TN and SRP:TP.

2.2.2 Time series standardization

To standardize the different measurement dates and the varying number of measurements per year (ranging from 9 to 35), we selected 9 reference days per year, separated by equal intervals of 29 days (Table 2). The number of reference days matches both the minimum number of measurements per year and the number of months covered per year (March to November). Based on the values at the individual measurement days, we linearly interpolated the log-transformed $\alpha_{realized}$, Chl-a, TP, SRP, TN, DIN, TN:TP, DIN:TN, SRP:TP, and Q, and the untransformed T_{water} and PAR at the reference days for each covered year. We obtained averaged seasonal cycles for individual stations by calculating the median per station and reference day. We note that when we refer to months in the following, they are always represented by these reference days.

https://doi.org/10.5194/egusphere-2026-830
Preprint. Discussion started: 28 April 2026

Table 2. Reference days for which water quality data was interpolated from measurements.

Day of the year	Date
77.0	March 18
106.125	April 16
135.25	May 15
164.375	June 13
193.5	July 12
222.625	August 10
251.75	September 8
280.875	October 7
310.0	November 6

2.2.3 Classification of seasonal patterns and comparison to drivers

To categorize the stations in our dataset by their seasonal patterns of $\alpha_{realized}$, we applied a k-means clustering algorithm from the *Python* library *scikit-learn* to the 133 averaged seasonal cycles of $\alpha_{realized}$ described above. The nine covered months (Table 2) served as the clustering dimensions. Based on an elbow plot (Supplementary Figure S1), we identified an optimal number of five clusters. In order to characterize the clusters, we subsequently calculated an average temporal coefficient of variation ($\overline{CV_t}$) as the ratio of the standard deviation and the mean of all $\alpha_{realized}$ values across months and stations for each cluster.

We visually assessed the seasonal patterns of the five clusters using sequences of boxplots, with the boxplots representing the distribution of $\alpha_{realized}$ per month across stations. This assessment was complemented by Mann-Whitney U tests, comparing the $\alpha_{realized}$ distributions of consecutive months within each cluster for statistically significant differences using a significance level of 0.05 (*stats* module, *Python* library *SciPy*). For each cluster, the month with the highest median value and all months that did not differ significantly from it in terms of their $\alpha_{realized}$ distribution were defined as peak months. Further, the median of these peak months was calculated per cluster, together with an all-year median covering all nine months. Additionally, the ratio of the peak median to the all-year median was calculated.

For the other temporally variable parameters, we created equivalent boxplot sequences grouped by the same clusters. $\overline{CV_t}$, peak-months medians, all-year medians, and peak-to-all-year ratios were also calculated for Chl-a. Further, we calculated station-wise Spearman rank correlation coefficients between the individual estimates of $\alpha_{realized}$ and the temporally variable physical parameters PAR, T_{water}, and Q, and between Chl-a and TN, TP, PAR, T_{water}, and Q. For each parameter and cluster, we assessed the median, 25th- and 75th-percentiles, and minimum and maximum values of the resulting correlation coefficients ($r_{\text{Parameter 1, Parameter 2}}$).We also determined the fraction of stations with a significant correlation (0.05 significance level). We note that significance is affected by the limited number of data points per station (n = 9).

https://doi.org/10.5194/egusphere-2026-830
Preprint. Discussion started: 28 April 2026

The distributions of river network properties and catchment characteristics for each cluster were compared through visual assessment of boxplots and additional Mann-Whitney U tests for statistical significance.

3 Results

3.1 Archetypal seasonal patterns

Among the 133 stations in the dataset, we identified five clusters (A, B, C, D, and E in the following), which differ in the overall magnitude of $\alpha_{realized}$ and their seasonal patterns (Figure 3, Table 3). Clusters were sorted by their $\overline{CV_t}$ of $\alpha_{realized}$ starting from the temporally least variable cluster A to the temporally most variable cluster E (Table 3). The seasonal patterns of Chl-a within the same five clusters are also displayed in Figure 3. The relationship among TP, Chl-a, and $\alpha_{realized}$ by month and cluster is illustrated by Supplementary Figure S2, showing that higher $\alpha_{realized}$ is reflected by higher Chl-a concentrations at a given TP concentration.

Cluster A, which has the lowest seasonal variability of $\alpha_{realized}$, is characterized by highest all-year median $\alpha_{realized}$ (Table 3). There are no significant changes between months, so no distinct peak month of $\alpha_{realized}$ was identified. Visually, a lower $\alpha_{realized}$ in May and June was noted compared to the rest of spring and summer, together with an overall broader range in autumn. In contrast to $\alpha_{realized}$, the Chl-a concentration shows a clear seasonal pattern with a maximum in late summer and early autumn. However, Chl-a levels remain high throughout the year, the all-year median (Figure 3, Table 3) consistently exceeds the phytoplankton bloom threshold of 30 $\mu g/l$ (taken from Dodds et al., 1998). All stations in cluster A are located either in the Elbe basin or the Baltic Sea tributaries (Figure 3, Supplementary Figure S3).

Although cluster B is the cluster with the second lowest seasonal variability of $\alpha_{realized}$, it displays significant decreases in $\alpha_{realized}$ from April to June and from October to November, resulting in a spring peak from March to April. The peak median $\alpha_{realized}$ of these months is two times lower than the all-year median of cluster A. For the rest of the year, $\alpha_{realized}$ of cluster B remains mostly constant with no significant changes from June to October. Similar to cluster A, Chl-a shows a peak during this period while $\alpha_{realized}$ remains constant. As a result, Chl-a shows two peaks, with no significant differences between March/April and September/August (Figure 3, Table 3). Cluster B stations are found in all four regions (Figure 3), but represent the highest fraction of clusters in the Elbe basin (32%, Supplementary Figure S3).

Cluster C is characterized by a significant spring increase in $\alpha_{realized}$, followed by a plateau from May to August. This summer plateau is two times higher than the peak of cluster B, but lower than the all-year median of cluster A. From August to November, $\alpha_{realized}$ of cluster C decreases steadily. The Chl-a pattern is similar, but variability between stations in a given month is slightly higher (Figure 3). The Chl-a plateau is longer, ranging from April to September. During this period, median Chl-a exceeds the phytoplankton bloom threshold. The stations of cluster C are mainly located in the Elbe basin and the Baltic Sea tributaries (Figure 3, Supplementary Figure S3).

Cluster D has of all clusters the lowest all-year median $\alpha_{realized}$, which is ten times smaller than the largest one in cluster A (Table 3). The $\alpha_{realized}$ peak of cluster D occurs in April, significantly exceeding the $\alpha_{realized}$ of March. From spring to summer, $\alpha_{realized}$ declines significantly between April and May and between May and June. From June to September,

https://doi.org/10.5194/egusphere-2026-830
Preprint. Discussion started: 28 April 2026

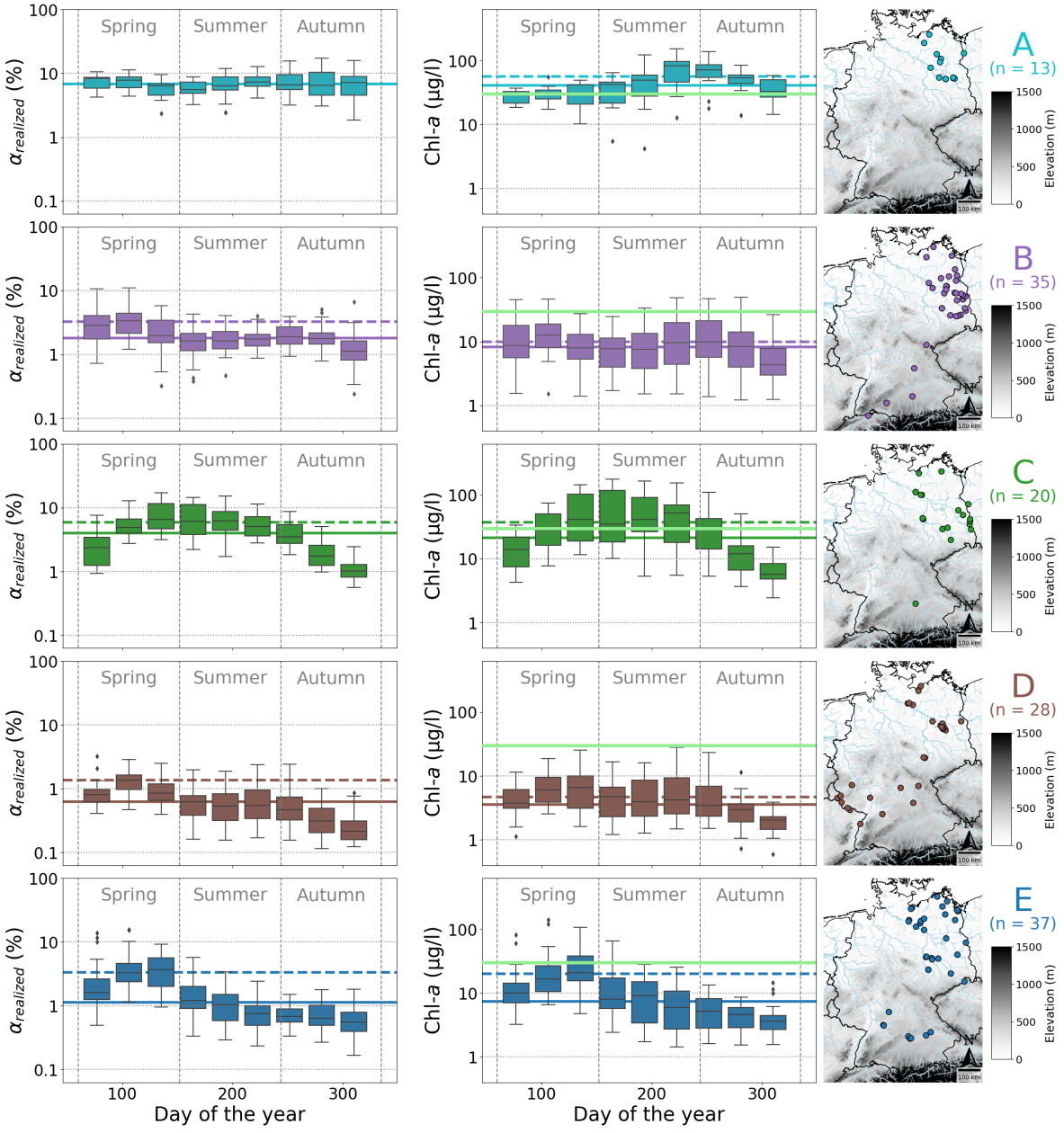

Figure 3. Five clusters (A-E) representing different archetypal seasonal patterns of $\alpha_{realized}$. The left column shows boxplots of monthly (March to November) $\alpha_{realized}$ for all stations assigned to each cluster, the middle column shows boxplots of the corresponding Chl-a concentrations. In both columns, the solid lines show the all-year medians of the clusters and the dashed line the peak medians (Table 3). In the Chl-a panels, the additional line in light green marks a threshold of 30 µg/l indicating phytoplankton blooms (Dodds et al., 1998). The right column displays the number of stations in each cluster and their locations in Germany.

https://doi.org/10.5194/egusphere-2026-830
Preprint. Discussion started: 28 April 2026

Table 3. Summary statistics of $\alpha_{realized}$ and Chl-a the five $\alpha_{realized}$-based seasonal clusters. Peak months are the month with the highest median value and all months not significantly differing from it. Bloom fractions are the fraction of Chl-a concentrations exceeding a threshold of 30 µg/l for phytoplankton blooms (Dodds et al., 1998).

Cluster	A	B	C	D	E
$n_{stations}$	13	35	20	28	37
$n_{QUADICA}$	3	16	7	16	16
$\alpha_{realized}$					
$\overline{CV_t}$	0.32	0.50	0.56	0.64	0.80
Peak months	Mar-Nov	Mar-Apr	May-Aug	Apr	Apr-May
Peak-months median	6.82%	3.23%	5.91%	1.36%	3.34%
All-year median	6.82%	1.81%	3.98%	0.63%	1.13%
Peak-to-all-year ratio	1.0	1.8	1.5	2.2	3.0
Chl-a					
$\overline{CV_t}$	0.48	0.49	0.63	0.58	0.74
Peak months	Jul-Oct	Mar-Apr, Aug-Sep	Apr-Sep	Mar-Sep	Apr-May
Peak-months median	56.91 µg/l	9.97 µg/l	37.48 µg/l	4.63 µg/l	19.91 µg/l
All-year median	40.73 µg/l	8.25 µg/l	21.36 µg/l	3.53 µg/l	7.43 µg/l
Peak-to-all-year ratio	1.4	1.2	1.8	1.3	2.7
Peak bloom fraction	82.7%	10.0%	57.5%	0.0%	27.0%
All-year bloom fraction	65.0%	5.4%	40.6%	0.0%	7.8%

$\alpha_{realized}$ remains low with no significant difference between months before decreasing significantly until November. Chl-a concentrations also decrease in autumn, but there is no significant peak in April (Figure 3). All individual Chl-a concentrations in cluster D are below the phytoplankton bloom threshold of 30 µg/l. Stations in this cluster are found in all regions except the Danube basin. They are particularly common in the Rhine basin, constituting more than two-thirds of the stations there (Figure 3, Supplementary Figure S3).

The seasonal $\alpha_{realized}$ pattern in cluster E is similar to that of cluster D, but with a spring peak from April to May twice as high. This peak is followed by a sharp, significant decrease from May to June. In summer and autumn, $\alpha_{realized}$ remains low, mostly below the all-year median with significant decreases from July to August and from October to November. The peak median $\alpha_{realized}$ is three times higher than the all-year median $\alpha_{realized}$, constituting the highest peak-to-all-year ratio and the highest $\overline{CV_t}$ of all five clusters (Table 3). The Chl-a pattern is the same, with April and May as the two peak months (Figure 3). Here, peak median Chl-a is slightly lower than the phytoplankton bloom threshold with more than a quarter of concentrations exceeding it. Cluster E stations are distributed across Germany with the highest fraction in the Danube basin, constituting almost two-thirds of the stations there (Figure 3, Supplementary Figure S3).

https://doi.org/10.5194/egusphere-2026-830
Preprint. Discussion started: 28 April 2026

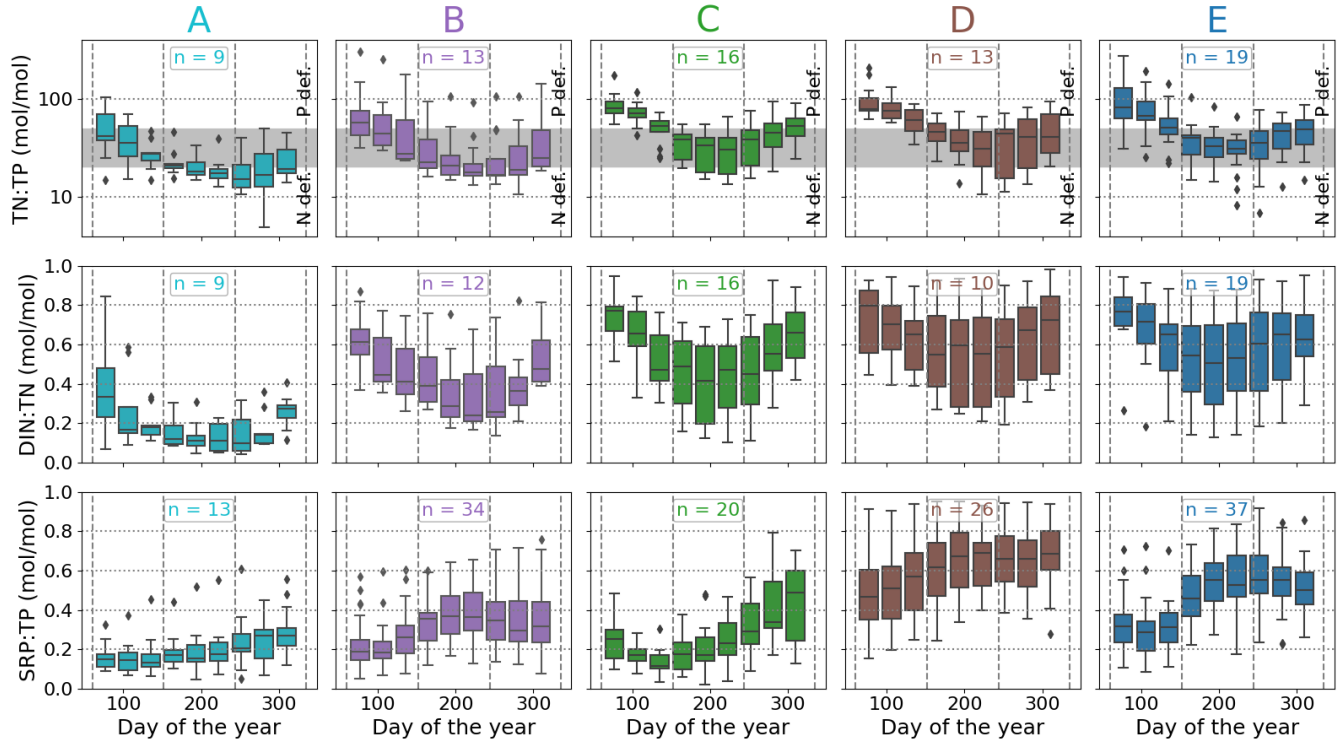

Figure 4. From top row to bottom row: Cluster-wise boxplots of the molar ratios TN:TP, DIN:TN, and SRP:TP per month. In the top row, the gray area marks the range $20 \leq$ TN:TP ≤ 50 indicating N and P co-deficiency while TN:TP < 20 indicates N deficiency only and TN:TP > 50 P deficiency only (Guildford and Hecky, 2000; Graeber et al., 2024).

3.2 Nutrient seasonality, stoichiometry, and reactive fractions

Both the nutrient TP, which is, together with Chl-a, directly linked to $\alpha_{realized}$ (Equation 3), and the nutrient TN show seasonal patterns that are mostly similar across clusters (Supplementary Figure S4). TP concentrations are highest in the summer months, although differences between months are in most cases insignificant. Across all months, cluster B has the lowest TP concentrations and cluster D the highest (Supplementary Figure S4, Supplementary Figure S5). In contrast, TN concentrations are mostly lowest in summer and have their maximum either in early spring or late autumn. Only in cluster A, TN has its peak in August (Supplementary Figure S4). Overall, TN concentrations of clusters A and B are significantly lower than TN concentrations of clusters C, D, and E (Supplementary Figure S5).

All five clusters display a similar seasonal pattern of TN:TP stoichiometry, with the highest ratios in spring, the lowest ratios in summer, and again relatively high ratios in autumn (Figure 4). However, cluster A consistently maintains lower TN:TP ratios throughout the year compared to the other four clusters (Supplementary Figure S6). Cluster B also has lower ratios than clusters C, D, and E, which, in contrast, are not significantly different from each other. Most TN:TP data for clusters A, B, C, and E fall within the N and P co-deficiency range while the majority of cluster D is in the P deficiency range (Supplementary Table S1).

https://doi.org/10.5194/egusphere-2026-830
Preprint. Discussion started: 28 April 2026

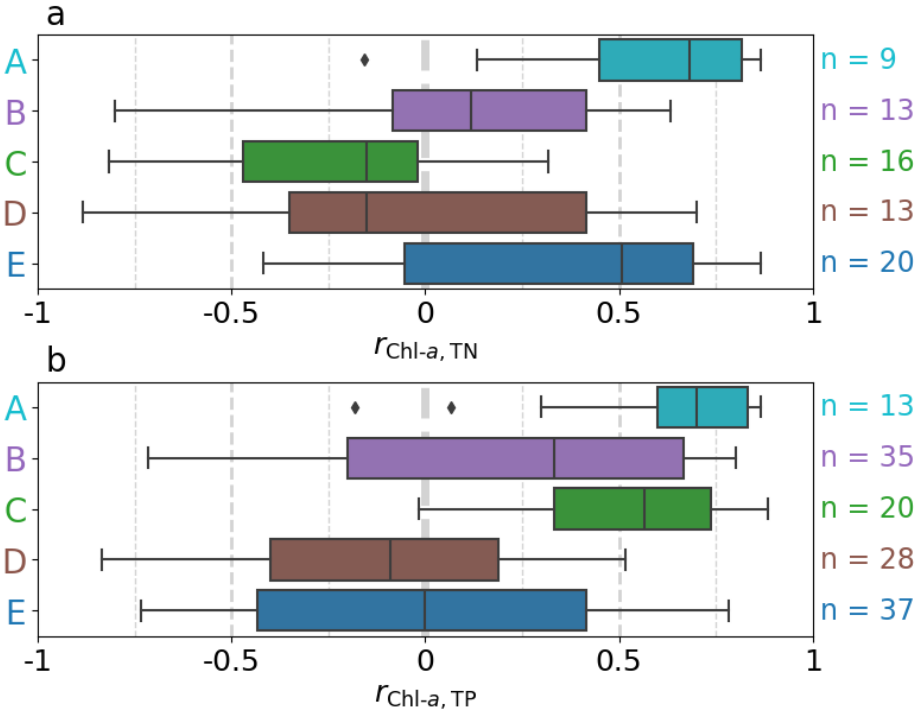

Figure 5. Cluster-wise distribution of the station-wise Spearman rank correlation coefficients (a) between Chl-a and TN, and (b) between Chl-a and TP.

In spring, clusters C, D, and E are predominantly in the P deficiency range, whereas clusters A and B have the highest fraction in the N deficiency range from July to October (or to November for cluster A).

The reactive nutrient fractions DIN:TN and SRP:TP are consistently lowest in cluster A, with a slight increase in SRP:TP over the year and slightly higher DIN:TN in early spring and late autumn compared to summer (Figure 4). The other clusters all have significantly lower SRP:TP in spring than during the rest of the year. In clusters B and C, the spring minimum of SRP:TP is as low as in cluster A, but both show a stronger increase during summer. While spring SRP:TP in cluster E is only slightly higher than in clusters A, B, and C, it increases much more sharply from May to June than in the other clusters. Cluster D has overall much higher SRP:TP in spring. DIN:TN in Clusters B, C, D, and E show similar seasonal patterns like cluster A but are generally much higher, with cluster B having the lowest values in summer.

In cluster A, both TP and TN correlate significantly with Chl-a at more than half of the stations (Figure 5, Supplementary Table S2). The median correlation coefficients of cluster A are $r_{\text{Chl-}a,\text{TP}} = 0.70$ and $r_{\text{Chl-}a,\text{TN}} = 0.68$. The median correlation coefficients $r_{\text{Chl-}a,\text{TP}} = 0.57$ in cluster C and $r_{\text{Chl-}a,\text{TN}} = 0.51$ in cluster E are also comparably high. However, they show a much broader range of correlation coefficients with less correlations being significant (Figure 5, Supplementary Table S2).

https://doi.org/10.5194/egusphere-2026-830
Preprint. Discussion started: 28 April 2026

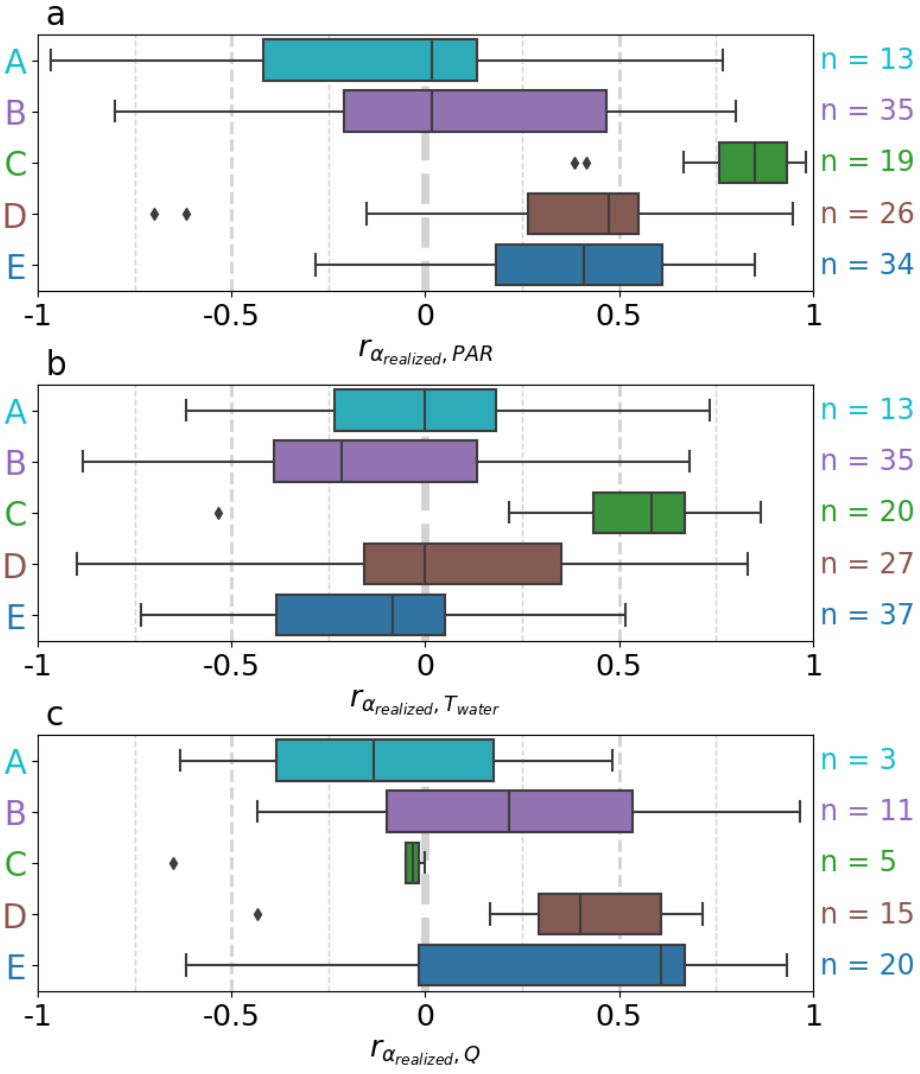

Figure 6. Cluster-wise distribution of the station-wise Spearman rank correlation coefficients at single stations (a) between $\alpha_{realized}$ and PAR, (b) between $\alpha_{realized}$ and T_{water}, and (c) between $\alpha_{realized}$ and Q.

3.3 Light, water temperature, and discharge

The correlation analysis of $\alpha_{realized}$ and the dynamic physical parameters PAR, T_{water}, and Q (Figure 6, Supplementary Table S3, seasonal patterns in Supplementary Figure S7) revealed only one cluster with consistently high station-wise correlations: The median correlation coefficient of $\alpha_{realized}$ and PAR of all stations in cluster C is high ($r_{\alpha_{realized},PAR}$ = 0.85) with 17 of 19 stations (89.5%) exhibiting a significant correlation (Supplementary Table S3). All other cluster-parameter combinations have no more than 40% of significant correlations. Other elevated median correlation coefficients include $r_{\alpha_{realized},T_{water}}$ = 0.58

https://doi.org/10.5194/egusphere-2026-830
Preprint. Discussion started: 28 April 2026

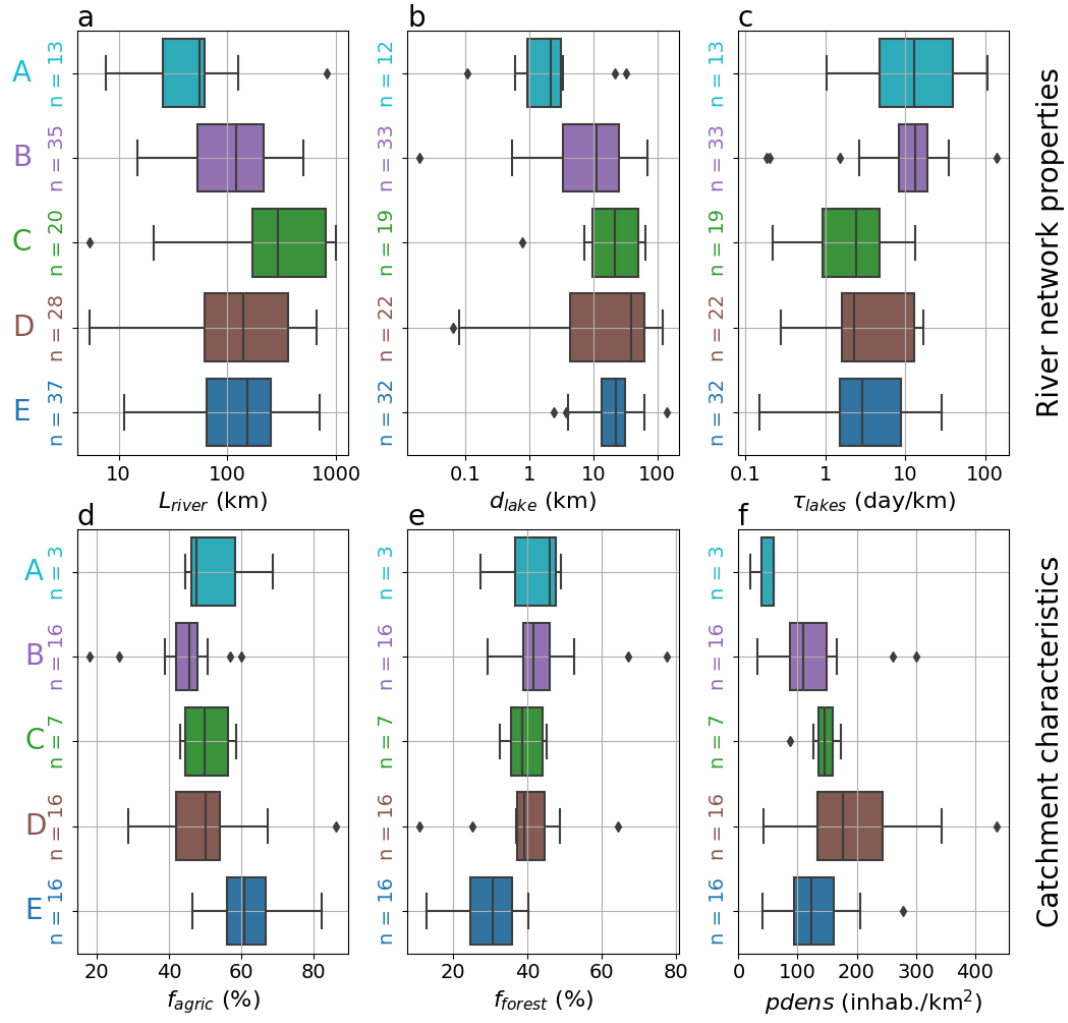

Figure 7. Box plots of the static river network properties and catchment characteristics for stations of the five clusters of seasonal $\alpha_{realized}$ patterns: (a) river length L_{river}, (b) distance to the nearest upstream lake d_{lake}, (c) lake residence time density τ_{lakes}, (d) forested land cover fraction f_{forest}, (e) agricultural land cover fraction f_{agric}, and (f) population density $pdens$. Numerical values are provided in Supplementary Table S5.

in cluster C, $r_{\alpha_{realized},PAR} = 0.48$ and $r_{\alpha_{realized},Q} = 0.40$ in cluster D, and $r_{\alpha_{realized},PAR} = 0.41$ and $r_{\alpha_{realized},Q} = 0.61$ in cluster E. Most of these parameter-cluster combinations, however, cover a broad range of correlation coefficients, including some with opposite signs (Figure 6). Correlation coefficients of PAR, T_{water}, and Q with Chl-a mostly show patterns similar to the ones with $\alpha_{realized}$ (Supplementary Figure S8, Supplementary Table S4).

https://doi.org/10.5194/egusphere-2026-830
Preprint. Discussion started: 28 April 2026

3.4 River network properties and catchment characteristics

Static river network properties L_{river}, d_{lake}, and τ_{lakes} differed significantly among clusters (Figure 7, Supplementary Figure S9). Cluster C is characterized by significantly larger river lengths L_{river} (median: 295 km, Supplementary Table S5) than the other clusters. In contrast, cluster A features the smallest L_{river} (median: 56 km) and the shortest distances to the nearest upstream lake d_{lake} (median: 2.07 km). Both clusters A and B showed significantly higher lake residence time densities τ_{lakes} than the other clusters, while the difference among them is not significant.

While cluster E is not clearly distinguishable from cluster D by river network properties, it has significantly different land cover fractions compared to clusters B, C, and D (Figure 7, Supplementary Figure S9). This includes significantly higher agricultural land cover fractions f_{agric} (median: 61%, Supplementary Table S5) and, conversely, significantly lower forested land cover fractions f_{forest} (median: 31%). Cluster D is characterized by the highest population density $pdens$ (median: 176.6 $\mathrm{inhabitants/km^2}$), significantly exceeding clusters A, B, and E. The lowest population densities were found in cluster A (median: 59.1 $\mathrm{inhabitants/km^2}$), where, however, catchment characteristics were only available for three stations.

4 Discussion

Based on 133 sites in a strongly human-impacted landscape, we identified five clusters with distinct seasonal patterns of the degree of realized eutrophication, $\alpha_{realized}$ (Figure 3). Within the five clusters, we identified three underlying seasonal patterns that are to different degrees and with partial overlaps visible across clusters. These patterns comprise (1) constant $\alpha_{realized}$ throughout the year in strongly lake-impacted rivers (clusters A and B), (2) high plateaus spanning spring and summer in mostly long rivers (cluster C), and (3) distinct spring peaks of variable magnitude in short to mid-sized rivers (clusters D and E, partly in cluster B). In the following, we discuss in detail the potential processes that explain the observed seasonal patterns and conclude with implications for river management.

4.1 Nutrients drive phytoplankton dynamics in lake-influenced rivers

Clusters A and B share a relatively constant $\alpha_{realized}$ throughout the year (Figure 3). Their TN:TP ratios indicate P and N co-deficiency or N deficiency, and their reactive nutrient fractions SRP:TP and DIN:TN (Figure 4) are comparably low. In cluster A, TP and TN further exhibit high positive correlations with Chl-a (Figure 5). Both clusters A and B do not show any consistent correlation with the physical factors (Figure 6) while lake residence time density τ_{lakes} is consistently higher compared to other clusters (Figure 7c). These results suggest that the constant seasonal $\alpha_{realized}$ pattern mainly reflects lake processes in which Chl-a concentrations are determined by nutrients rather than by physical factors.

Cluster A differs from cluster B by having higher and more constant $\alpha_{realized}$, lower reactive nutrient fractions, and shorter L_{river} and d_{lake} (Figure 7a-b). We argue that cluster A reflects the seasonal $\alpha_{realized}$ pattern characteristic of upstream lakes in our dataset while cluster B shows a weaker form mixed with in-stream patterns that cause elevated $\alpha_{realized}$ in spring (Figure 3) as discussed below. This agrees with the findings of Hubig et al. (2025), who found particularly high station medians of

https://doi.org/10.5194/egusphere-2026-830
Preprint. Discussion started: 28 April 2026

$\alpha_{realized}$ when both L_{river} and d_{lake} are short. They argue that the effect of lakes decreases with increasing distance due to enhanced grazing by benthic filter feeders close to the lake outlet (Welker and Walz, 1998) and a dilution effect when the river is longer and thus has more lake-free tributaries.

As $\alpha_{realized}$ is mostly constant in cluster A, the physical factors PAR, T_{water}, and Q with their distinct seasonal patterns (Supplementary Figure S7) do not appear to affect the efficiency of phytoplankton biomass in incorporating P. Instead, Chl-a and TP concentrations show very similar seasonal patterns with a consistently high positive correlation (Figure 5b, Supplementary Figure S4), indicating that TP is utilized with constant efficiency throughout the entire vegetation period. Especially in spring and autumn, the role of light seems less important in cluster A compared to other clusters (Supplementary Figure S7), although light likely limits phytoplankton growth here during the winter months not covered in this study (Sommer et al., 1986, 2012).

The constant $\alpha_{realized}$ in cluster A raises the question why the median does not approach 100% - the theoretical limit of P for phytoplankton growth. We argue that this could be a result of co-limitation by N, which is supported by the observed TN:TP ratios (Figure 4) and the positive correlations between Chl-a and both TP and TN concentrations (Figure 5). In addition, reactive nutrient fractions SRP:TP and DIN:TN of cluster A are both comparably low during almost the entire covered period (Figure 4), contrasting the other clusters that are also in the co-deficiency or N deficiency range of TN:TP. This further supports that in cluster A, phytoplankton growth is controlled by both P and N.

As an additional explanation for missing $\alpha_{realized}$ values close to 100%, we note that standardizing the data (interpolating values on the nine reference days and averaging over all measurement years, Section 2.2.2) can smooth out short-term variations, which in the raw data sometimes produce higher $\alpha_{realized}$ values (Figure 2). Furthermore, we acknowledge that phytoplankton communities are likely to vary spatially and temporally, leading to variable Chl-a content per biomass (Riemann et al., 1989). Therefore, there is uncertainty in the upper biomass limit that serves as the baseline for $\alpha_{realized}$, though we believe that species-dependent variability in $\alpha_{realized}$ contributes only minimally to the strong spatial and temporal $\alpha_{realized}$ variations observed in our data. Further, we argue that the transition between clusters A and B are gradual so that the mechanisms lowering $\alpha_{realized}$ in cluster B compared to cluster A are, to a lower degree, valid for cluster A as well, potentially leading to lower $\alpha_{realized}$ downstream of the outlet than directly in a lake. We note that particularly for cluster B, DIN and TN coverage are rather low (12 out of 35 stations, Figure 4, Table 3), which limits mechanistic interpretation for this cluster. However, cluster A is well-represented (9 out of 13 stations) and strongly supports the combined effect of both TP and TN on phytoplankton growth in lake-influenced rivers.

4.2 Light control and loss processes in lake-free rivers

The clusters C, D, and E display more pronounced seasonal changes in $\alpha_{realized}$ than clusters A and B (Figure 3). This is evident from the observed increases and decreases of $\alpha_{realized}$ during spring and autumn as well as from overall higher correlations with the physical parameters PAR, T_{water}, and Q (Figure 6). Particularly the high correlation between $\alpha_{realized}$ and PAR in cluster C suggests that its summer plateau is mainly driven by light. However, the contrasting low values of

https://doi.org/10.5194/egusphere-2026-830
Preprint. Discussion started: 28 April 2026

$\alpha_{realized}$ in summer for clusters D and E cannot be directly explained by the physical parameters, which exhibit similar patterns across all clusters.

We argue that loss processes are a likely explanation for the low summer $\alpha_{realized}$ in clusters D and E. They are potentially facilitated by grazing through invasive and native benthic filter-feeders, such as *Corbicula* spp. or *Dreissena* spp., which have already been identified as potential factors lowering $\alpha_{realized}$ (Hubig et al., 2025). The observed seasonal pattern of clusters D and E supports this explanation as grazing by benthic filter-feeders has been suggested to contribute to the decline of phytoplankton spring peaks (e.g., Welker and Walz, 1998; Weitere and Arndt, 2002; Pigneur et al., 2014; Hardenbicker et al., 2016). For the low $\alpha_{realized}$ in summer, the observed sensitivity of grazers to water temperature is probably crucial as filtration rates increase with water temperature between 8°C and 20°C (Lei et al., 1996), matching the seasonal patterns of T_{water} observed in our dataset (Supplementary Figure S7). Together with known filter feeder biomass maxima in summer (Pigneur et al., 2014), this is consistent with the decrease of $\alpha_{realized}$ that we observe from April and May to June, indicating that loss processes exceed phytoplankton growth. The timing also matches findings from Pigneur et al. (2014), who found lower summer-to-spring ratios in Chl-a when filter-feeders were included in their model. We note that with its moderate spring peak, cluster B is also likely to be influenced by grazing in addition to the nutrient-controlled lakes processes (cluster A, section 4.1).

Cluster C differs from the other clusters by its significantly longer L_{river} (Figure 7a, Supplementary Figure S9a). We note that the Elbe river is overrepresented among the long rivers of our dataset. As the Elbe river has low abundances of benthic filter-feeders compared to rivers of similar size (Hardenbicker et al., 2016), the significantly higher L_{river} values in cluster C may also be due to a bias of the dataset. Alternatively, since phytoplankton species with different temperature-dependent growth rates typically succeed the spring peak-forming species in summer (Garnier et al., 1995), there may also be a change in sensitivity to water residence time, leading to the observed diverging values of $\alpha_{realized}$ in summer between longer and shorter rivers. As data on grazer abundances and phytoplankton species are lacking in our dataset, a clear disentanglement of these effects is not possible.

4.3 Land cover and point source impacts on river eutrophication

While both clusters D and E exhibit peaks of $\alpha_{realized}$ in spring, these peaks differ in magnitude and timing despite similar river lengths and lake influences. In contrast, the two clusters differ significantly in their agricultural and forested land cover fractions f_{agric} and f_{forest}, implying that $\alpha_{realized}$ in spring is modulated by land use.

Spring peaks in rivers are typically triggered by increased light availability, resulting from a spring decrease in discharge and an increase in solar radiation (Garnier et al., 1995; Hardenbicker et al., 2014). As we observe both a decrease in Q and an increase in PAR in spring (Supplementary Figure S7), this can explain the presence of spring peaks in both clusters. However, we argue that effective light availability differs between clusters D and E, with the more forested catchments in cluster D providing stronger riparian shading than the more agricultural catchments in cluster E (Figure 7), thereby modulating the magnitude and duration of the spring peaks. While both clusters show a significant increase in $\alpha_{realized}$ from March to April, cluster E remains at a high level and only shows a sharp decrease after May, whereas cluster D already decreases significantly after April. The lower spring peak in cluster D is consistent with stronger riparian shading, which has been shown to efficiently

https://doi.org/10.5194/egusphere-2026-830
Preprint. Discussion started: 28 April 2026

reduce phytoplankton growth in rivers (Hutchins et al., 2010). A link between land cover and riparian shading was also reported by Rode et al. (2016), who observed higher in-stream nutrient assimilation rates in an agricultural part of a catchment compared to a forested part. Accounting for the mitigating effect of increasing riparian leaf cover in April on these processes (Rode et al., 2016), differences in land cover also explain the earlier and more gradual decline from April to May in cluster D. We note that riparian shading primarily reduces light availability in headwaters, where channel widths are small. However, as these headwaters constitute a substantial portion of the upstream networks of mid-sized rivers, phytoplankton concentrations may also be limited further downstream.

Beyond the seasonal shape regulated by shading, we argue that the overall low level of $\alpha_{realized}$ in Cluster D is reinforced by anthropogenic factors. Cluster D, which exhibits the lowest $\alpha_{realized}$ (Figure 3, Supplementary Figure S5a), is also characterized by a significantly higher population density $pdens$ (Figure 7f, Supplementary Figure S9f) and higher all-year TP concentrations (Supplementary Figure S5c) compared to the other clusters. Here, the high population density suggests a high prevalence of TP inputs from point sources (Yang et al., 2019) in cluster D. With point sources rather near to the observation points, the effective residence time of TP may be shorter than expected from the river length and upstream lake influence, resulting in comparably low phytoplankton biomass at a given TP level. This effect has been described by Neal et al. (2006) and was demonstrated for a densely populated reach of the Rhine river by Hubig et al. (2025), and provides a plausible explanation for the low $\alpha_{realized}$ observed in cluster D.

4.4 Implications for river management

Our findings have implications for river management beyond reducing P inputs, comprising the following points: (1) the identification of river locations and times that are at high risk of developing phytoplankton blooms, (2) dual nutrient management of N and P, and (3) the role of riparian shading in preventing phytoplankton growth.

Our study revealed that the degree of realized eutrophication is particularly high near upstream lakes (cluster A) and in the lower reaches of long rivers without significant grazing (cluster C), which is in line with Hubig et al. (2025). This indicates that the available TP is efficiently converted into phytoplankton biomass, leading to a high risk of blooms (> 30 µg/l Chl-a) at these locations. Especially downstream of lakes, this high risk persists throughout the entire growing season, including March, October, and November (cluster A), but decreases with increasing distance to the lake and an overall larger upstream river network (cluster B). According to our findings, rivers without strong lake influence (cluster C, D, and E) are mostly free of critical Chl-a concentrations during March, October, and November, even at high TP levels (Supplementary Figure S2). From April to September, long rivers without grazing (cluster C) are, for the most part, as efficient to make use of TP for phytoplankton growth as rivers of cluster A, and hence are at similar risk for phytoplankton blooms (Figure 3, Table 3). For short to mid-sized rivers that are affected by loss processes in summer and, at the same time, less controlled by riparian shading (cluster E), we highlight an elevated risk of phytoplankton blooms in spring. Although these rivers have low all-year median Chl-a concentrations, 27% of the observations in April and May exceed the critical threshold for phytoplankton blooms (Figure 3, Table 3).

https://doi.org/10.5194/egusphere-2026-830
Preprint. Discussion started: 28 April 2026

For the river locations at highest risk (clusters A and C), nutrient management remains an important measure to prevent phytoplankton blooms. We argue that for these locations, N management is as important as P management. This is particularly true for the lake-impacted cluster A, where N deficiency may even be more dominant than P deficiency. N management could be especially important at locations with elevated phytoplankton levels in summer (cluster C) as TN:TP ratios then tend to fall within the co-deficiency range. This implication is supported by the increasing frequency of reported summer blooms in recent years even in rivers that previously exhibited only spring blooms (e.g., Kleinteich et al., 2024), indicating more favorable physical conditions for phytoplankton growth in summer due to climate change. These summer blooms under hot conditions require special attention as they provide particularly good conditions for harmful cyanobacteria (Paerl and Huisman, 2008; Kleinteich et al., 2024). If the TN:TP ratio is in the co-deficiency range, reducing TN would lower the TP-based $\alpha_{realized}$, allowing for reduced Chl-a concentrations without changing TP.

As an additional measure beyond nutrient reduction, the observed significant differences between forested and agricultural catchments in the spring peak (clusters D and E, Figure 7) support the use of riparian shading, as suggested in earlier studies (Hutchins et al., 2010; Bowes et al., 2012b). Reducing $\alpha_{realized}$ through shading would be an addition to lowering TP concentrations to decrease Chl-a concentrations (Figure 2, Supplementary Figure S2). While our study provides evidence only for the effect of differing land covers (i.e., f_{forest} versus f_{agric}) on short and mid-sized rivers (clusters D and E), longer rivers may also benefit from shading along their shorter tributaries. In contrast, phytoplankton growth in lakes (cluster A) is unlikely to be significantly reduced by riparian shading as the canopy height at the lake shore has only a limited effect on light availability.

5 Conclusions

In this study, we investigated the seasonal dynamics of the phosphorus-incorporation efficiency of river phytoplankton, quantified by the degree of realized eutrophication $\alpha_{realized}$. We analyzed a water quality dataset covering 133 river locations across different drainage basins and stream orders in a strongly human-impacted landscape in Germany. Among these stations, we identified five clusters exhibiting distinct archetypal seasonal dynamics of $\alpha_{realized}$ revealing three partly overlapping patterns with different underlying mechanistic explanations:

(1) River locations strongly influenced by upstream lakes tend to have consistently high $\alpha_{realized}$, low reactive nutrient fractions, and high TN-Chl-a and TP-Chl-a correlations, suggesting that phytoplankton concentrations are limited by both N and P (Clusters A and B, 36.1% of all stations). This pattern is weakened but still visible when the distance to the upstream lake or lakes is greater. (2) Long rivers, dominated by the Elbe river in our dataset, often show a clear seasonal pattern of $\alpha_{realized}$ with a maximum during the summer months (Cluster C, 15.0% of all stations). The high correlation with photosynthetically active radiation indicates that light availability predominantly controls their seasonal pattern, with little evidence of efficient phytoplankton loss through grazers. (3) Short to mid-sized rivers without lake influence typically show only a spring peak in $\alpha_{realized}$, with low values in summer and autumn (Clusters D and E, 48.9% of all stations). We attributed the post-spring peak decrease in $\alpha_{realized}$ to enhanced loss rates in summer due to grazing by benthic filter-feeders. The timing and magnitude of the spring peak differ among catchments with different forested and agricultural land cover fractions, leading us to conclude

https://doi.org/10.5194/egusphere-2026-830
Preprint. Discussion started: 28 April 2026

that riparian shading can significantly subdue the spring peak. Additionally, we acknowledged that P point sources near the measurement stations in densely populated catchments can lead to lower $\alpha_{realized}$ than suggested by river network properties, which potentially affects rivers across all three patterns.

We concluded that there is a high risk of phytoplankton blooms from early spring to late autumn at river locations very close to upstream lakes and from mid-spring to early autumn in long rivers without significant loss processes. Rivers with high phytoplankton loss in summer due to grazing may still experience critical phytoplankton concentrations in spring if they are less shaded. For locations prone to high phytoplankton concentrations in summer, we found N management to be as important as P management. Instead of only lowering nutrients, rivers could additionally be managed by targeted riparian shading, reducing Chl-a concentrations by physically lowering $\alpha_{realized}$.

Data availability. The observational water quality data are largely part of the QUADICA database (Ebeling et al., 2022, 2026). All original water quality data were provided by German environmental authorities, including for stations not included in QUADICA. For details, refer to Hubig et al. (2025). The surface shortwave downwelling radiation used for PAR can be obtained from the Copernicus E-OBS (Copernicus Climate Change Service, 2020; Cornes et al., 2018).

Author contributions. AH: Conceptualization, Data curation, Formal analysis, Investigation, Methodology, Visualization, Writing (original draft preparation), Writing (review and editing); PE: Data curation, Investigation, Writing (review and editing); DG: Conceptualization, Writing (review and editing), US: Conceptualization, Data curation, Investigation, Methodology, Supervision, Writing (review and editing); AM: Conceptualization, Methodology, Supervision, Writing (review and editing).

Competing interests. The contact author has declared that none of the authors has any competing interests.

Acknowledgements. We thank the German environmental authorities for providing the data.

https://doi.org/10.5194/egusphere-2026-830
Preprint. Discussion started: 28 April 2026

References

Andersen, I. M., Taylor, J. M., Kelly, P. T., Hoke, A. K., Robbins, C. J., and Scott, J. T.: Nitrogen fixation may not alleviate stoichiometric imbalances that limit primary production in eutrophic lake ecosystems, Ecology, 106, e4516, https://doi.org/10.1002/ecy.4516, 2025.

Balbi, D. M.: Suspended chlorophyll in the River Nene, a small nutrient-rich river in eastern England: long-term and spatial trends, Science of the total environment, 251, 401–421, https://doi.org/10.1016/S0048-9697(00)00419-8, 2000.

Bowes, M., Gozzard, E., Johnson, A., Scarlett, P., Roberts, C., Read, D., Armstrong, L., Harman, S., and Wickham, H.: Spatial and temporal changes in chlorophyll-a concentrations in the River Thames basin, UK: are phosphorus concentrations beginning to limit phytoplankton biomass?, Science of the Total Environment, 426, 45–55, https://doi.org/10.1016/j.scitotenv.2012.02.056, 2012a.

Bowes, M., Ings, N., McCall, S., Warwick, A., Barrett, C., Wickham, H., Harman, S., Armstrong, L., Scarlett, P., Roberts, C., et al.: Nutrient and light limitation of periphyton in the River Thames: implications for catchment management, Science of the Total Environment, 434, 201–212, https://doi.org/10.1016/j.scitotenv.2011.09.082, 2012b.

Bowes, M., Loewenthal, M., Read, D., Hutchins, M., Prudhomme, C., Armstrong, L., Harman, S., Wickham, H., Gozzard, E., and Carvalho, L.: Identifying multiple stressor controls on phytoplankton dynamics in the River Thames (UK) using high-frequency water quality data, Science of the Total Environment, 569, 1489–1499, https://doi.org/10.1016/j.scitotenv.2016.06.239, 2016.

Copernicus Climate Change Service: E-OBS daily gridded meteorological data for Europe from 1950 to present derived from in-situ observations. Copernicus Climate Change Service (C3S) Climate Data Store (CDS), https://doi.org/10.24381/cds.151d3ec6, Accessed on 01-Oct-2022, 2020.

Cornes, R. C., Van Der Schrier, G., Van Den Besselaar, E. J., and Jones, P. D.: An ensemble version of the E-OBS temperature and precipitation data sets, Journal of Geophysical Research: Atmospheres, 123, 9391–9409, https://doi.org/10.1029/2017JD028200, 2018.

Davidson, K., Gowen, R. J., Harrison, P. J., Fleming, L. E., Hoagland, P., and Moschonas, G.: Anthropogenic nutrients and harmful algae in coastal waters, Journal of environmental management, 146, 206–216, https://doi.org/10.1016/j.jenvman.2014.07.002, 2014.

de Vries, W., Posch, M., Simpson, D., de Leeuw, F. A., van Grinsven, H. J., Schulte-Uebbing, L. F., Sutton, M. A., and Ros, G. H.: Trends and geographic variation in adverse impacts of nitrogen use in Europe on human health, climate, and ecosystems: A review, Earth-Science Reviews, 253, 104 789, https://doi.org/10.1016/j.earscirev.2024.104789, 2024.

Desortová, B. and Punčochář, P.: Variability of phytoplankton biomass in a lowland river: response to climate conditions, Limnologica, 41, 160–166, https://doi.org/10.1016/j.limno.2010.08.002, 2011.

Dodds, W. K. and Smith, V. H.: Nitrogen, phosphorus, and eutrophication in streams, Inland Waters, 6, 155–164, https://doi.org/10.5268/IW-6.2.909, 2016.

Dodds, W. K., Jones, J. R., and Welch, E. B.: Suggested classification of stream trophic state: distributions of temperate stream types by chlorophyll, total nitrogen, and phosphorus, Water research, 32, 1455–1462, https://doi.org/10.1016/S0043-1354(97)00370-9, 1998.

Ebeling, P., Dupas, R., Abbott, B., Kumar, R., Ehrhardt, S., Fleckenstein, J. H., and Musolff, A.: Long-term nitrate trajectories vary by season in Western European catchments, Global Biogeochemical Cycles, 35, e2021GB007 050, https://doi.org/10.1029/2021GB007050, 2021.

Ebeling, P., Kumar, R., Lutz, S. R., Nguyen, T., Sarrazin, F., Weber, M., Büttner, O., Attinger, S., and Musolff, A.: QUADICA: water QUAlity, DIscharge and Catchment Attributes for large-sample studies in Germany, Earth System Science Data, 14, 3715–3741, https://doi.org/10.5194/essd-14-3715-2022, 2022.

https://doi.org/10.5194/egusphere-2026-830
Preprint. Discussion started: 28 April 2026

Ebeling, P., Hubig, A., Wachholz, A., Scharfenberger, U., Haug, S., Nguyen, T., Sarrazin, F., Batool, M., Musolff, A., and Kumar, R.: QUADICA v2: extending the large-sample data set for water QUAlity, DIscharge and Catchment Attributes in Germany, Earth System Science Data, 18, 691–712, https://doi.org/10.5194/essd-18-691-2026, 2026.

Edwards, K. F., Klausmeier, C. A., and Litchman, E.: A three-way trade-off maintains functional diversity under variable resource supply, The American Naturalist, 182, 786–800, https://doi.org/10.1086/673532, 2013.

Edwards, K. F., Klausmeier, C. A., and Litchman, E.: Nutrient utilization traits of phytoplankton, Ecology, 96, 2311–2311, https://doi.org/10.1890/14-2252.1, 2015.

Friedrich, G. and Pohlmann, M.: Long-term plankton studies at the lower Rhine/Germany, Limnologica, 39, 14–39, https://doi.org/10.1016/j.limno.2008.03.006, 2009.

Garnier, J., Billen, G., and Coste, M.: Seasonal succession of diatoms and Chlorophyceae in the drainage network of the Seine River: Observation and modeling, Limnology and Oceanography, 40, 750–765, https://doi.org/10.4319/lo.1995.40.4.0750, 1995.

Gosselain, V., Viroux, L., and Descy, J.-P.: Can a community of small-bodied grazers control phytoplankton in rivers?, Freshwater Biology, 39, 9–24, https://doi.org/10.1046/j.1365-2427.1998.00258.x, 1998.

Graeber, D., Pusch, M. T., Lorenz, S., and Brauns, M.: Cascading effects of flow reduction on the benthic invertebrate community in a lowland river, Hydrobiologia, 717, 147–159, https://doi.org/10.1007/s10750-013-1570-1, 2013.

Graeber, D., McCarthy, M. J., Shatwell, T., Borchardt, D., Jeppesen, E., Søndergaard, M., Lauridsen, T. L., and Davidson, T. A.: Consistent stoichiometric long-term relationships between nutrients and chlorophyll-a across shallow lakes, Nature Communications, 15, 809, https://doi.org/10.1038/s41467-024-45115-3, 2024.

Guildford, S. J. and Hecky, R. E.: Total nitrogen, total phosphorus, and nutrient limitation in lakes and oceans: Is there a common relationship?, Limnology and oceanography, 45, 1213–1223, https://doi.org/10.4319/lo.2000.45.6.1213, 2000.

Ha, K., Kim, H.-W., and Joo, G.-J.: The phytoplankton succession in the lower part of hypertrophic Nakdong River (Mulgum), South Korea, Hydrobiologia, 369, 217–227, https://doi.org/10.1023/A:1017067809089, 1998.

Hardenbicker, P., Rolinski, S., Weitere, M., and Fischer, H.: Contrasting long-term trends and shifts in phytoplankton dynamics in two large rivers, International Review of Hydrobiology, 99, 287–299, https://doi.org/https://doi.org/10.1002/iroh.201301680, 2014.

Hardenbicker, P., Weitere, M., Ritz, S., Schöll, F., and Fischer, H.: Longitudinal Plankton Dynamics in the Rivers Rhine and Elbe, River Research and Applications, 32, 1264–1278, https://doi.org/https://doi.org/10.1002/rra.2977, 2016.

Hubig, A., Musolff, A., Shatwell, T., Weitere, M., Wachholz, A., Ebeling, P., and Scharfenberger, U.: Linking spatial patterns of chlorophyll a and phosphorus concentrations: River length and upstream lakes control realized eutrophication in German rivers, Water Research, p. 124372, https://doi.org/10.1016/j.watres.2025.124372, 2025.

Hutchins, M., Johnson, A., Deflandre-Vlandas, A., Comber, S., Posen, P., and Boorman, D.: Which offers more scope to suppress river phytoplankton blooms: reducing nutrient pollution or riparian shading?, Science of the Total Environment, 408, 5065–5077, https://doi.org/10.1016/j.scitotenv.2010.07.033, 2010.

Ibelings, B., Admiraal, W., Bijkerk, R., Ietswaart, T., and Prins, H.: Monitoring of algae in Dutch rivers: does it meet its goals?, Journal of applied phycology, 10, 171–181, https://doi.org/10.1023/A:1008049000764, 1998.

Istvánovics, V. and Honti, M.: Efficiency of nutrient management in controlling eutrophication of running waters in the Middle Danube Basin, Hydrobiologia, 686, 55–71, https://doi.org/10.1007/s10750-012-0999-y, 2012.

Julian, J., Doyle, M., and Stanley, E.: Empirical modeling of light availability in rivers, Journal of Geophysical Research: Biogeosciences, 113, https://doi.org/10.1029/2007JG000601, 2008.

https://doi.org/10.5194/egusphere-2026-830
Preprint. Discussion started: 28 April 2026

Kamjunke, N., Rode, M., Baborowski, M., Kunz, J. V., Zehner, J., Borchardt, D., and Weitere, M.: High irradiation and low discharge promote the dominant role of phytoplankton in riverine nutrient dynamics, Limnology and Oceanography, 66, 2648–2660, https://doi.org/10.1002/lno.11778, 2021.

Kleinteich, J., Frassl, M. A., Schulz, M., and Fischer, H.: Climate change triggered planktonic cyanobacterial blooms in a regulated temperate river, Scientific Reports, 14, 16 298, https://doi.org/10.1038/s41598-024-66586-w, 2024.

Köhler, J.: Origin and succession of phytoplankton in a river-lake system (Spree, Germany), Hydrobiologia, 289, 73–83, https://doi.org/10.1007/BF00007410, 1994.

Le Moal, M., Gascuel-Odoux, C., Ménesguen, A., Souchon, Y., Étrillard, C., Levain, A., Moatar, F., Pannard, A., Souchu, P., Lefebvre, A., et al.: Eutrophication: a new wine in an old bottle?, Science of the total environment, 651, 1–11, https://doi.org/10.1016/j.scitotenv.2018.09.139, 2019.

Lehner, B. and Grill, G.: Global river hydrography and network routing: baseline data and new approaches to study the world's large river systems, Hydrological Processes, 27, 2171–2186, https://doi.org/https://doi.org/10.1002/hyp.9740, 2013.

Lei, J., Payne, B. S., and Wang, S. Y.: Filtration dynamics of the zebra mussel, Dreissena polymorpha, Canadian journal of fisheries and aquatic sciences, 53, 29–37, https://doi.org/10.1139/f95-164, 1996.

Messager, M. L., Lehner, B., Grill, G., Nedeva, I., and Schmitt, O.: Estimating the volume and age of water stored in global lakes using a geo-statistical approach, Nature communications, 7, 13 603, https://doi.org/10.1038/ncomms13603, 2016.

Minaudo, C., Meybeck, M., Moatar, F., Gassama, N., and Curie, F.: Eutrophication mitigation in rivers: 30 years of trends in spatial and seasonal patterns of biogeochemistry of the Loire River (1980–2012), Biogeosciences, 12, 2549–2563, https://doi.org/10.5194/bg-12-2549-2015, 2015.

Mischke, U., Venohr, M., and Behrendt, H.: Using Phytoplankton to Assess the Trophic Status of German Rivers, International Review of Hydrobiology, 96, 578–598, https://doi.org/https://doi.org/10.1002/iroh.201111304, 2011.

Moon, D. L., Scott, J. T., and Johnson, T. R.: Stoichiometric imbalances complicate prediction of phytoplankton biomass in US lakes: Implications for nutrient criteria, Limnology and oceanography, 66, 2967–2978, https://doi.org/10.1002/lno.11851, 2021.

Mosisch, T. D., Bunn, S. E., and Davies, P. M.: The relative importance of shading and nutrients on algal production in subtropical streams, Freshwater biology, 46, 1269–1278, https://doi.org/10.1046/j.1365-2427.2001.00747.x, 2001.

Neal, C., Hilton, J., Wade, A. J., Neal, M., and Wickham, H.: Chlorophyll-a in the rivers of eastern England, Science of the Total Environment, 365, 84–104, https://doi.org/10.1016/j.scitotenv.2006.02.039, 2006.

Paerl, H. W. and Huisman, J.: Blooms like it hot, Science, 320, 57–58, https://doi.org/10.1126/science.1155398, 2008.

Paerl, H. W. and Otten, T. G.: Harmful cyanobacterial blooms: causes, consequences, and controls, Microbial ecology, 65, 995–1010, https://doi.org/10.1007/s00248-012-0159-y, 2013.

Pigneur, L.-M., Falisse, E., Roland, K., Everbecq, E., Deliège, J.-F., Smitz, J. S., Van Doninck, K., and Descy, J.-P.: Impact of invasive A sian clams, C orbicula spp., on a large river ecosystem, Freshwater Biology, 59, 573–583, https://doi.org/10.1111/fwb.12286, 2014.

Reynolds, C.: Hydroecology of river plankton: the role of variability in channel flow, Hydrological Processes, 14, 3119–3132, https://doi.org/10.1002/1099-1085(200011/12)14:16/17<3119::AID-HYP137>3.0.CO;2-6, 2000.

Reynolds, C., Descy, J.-P., and Padisák, J.: Are phytoplankton dynamics in rivers so different from those in shallow lakes?, Hydrobiologia, 289, 1 – 7, https://doi.org/10.1007/BF00007404, 1994.

Riemann, B., Simonsen, P., and Stensgaard, L.: The carbon and chlorophyll content of phytoplankton from various nutrient regimes, Journal of Plankton Research, 11, 1037–1045, https://doi.org/10.1093/plankt/11.5.1037, 1989.

https://doi.org/10.5194/egusphere-2026-830
Preprint. Discussion started: 28 April 2026

Rode, M., Halbedel ne´e Angelstein, S., Anis, M. R., Borchardt, D., and Weitere, M.: Continuous in-stream assimilatory nitrate uptake from high-frequency sensor measurements, Environmental science & technology, 50, 5685–5694, https://doi.org/10.1021/acs.est.6b00943, 2016.

Scharfenberger, U., Jeppesen, E., Beklioğlu, M., Søndergaard, M., Angeler, D. G., Çakıroğlu, A. İ., Drakare, S., Hejzlar, J., Mahdy, A., Papastergiadou, E., et al.: Effects of trophic status, water level, and temperature on shallow lake metabolism and metabolic balance: A standardized pan-European mesocosm experiment, Limnology and Oceanography, 64, 616–631, https://doi.org/10.1002/lno.11064, 2019.

Schwaderer, A. S., Yoshiyama, K., de Tezanos Pinto, P., Swenson, N. G., Klausmeier, C. A., and Litchman, E.: Eco-evolutionary differences in light utilization traits and distributions of freshwater phytoplankton, Limnology and Oceanography, 56, 589–598, https://doi.org/10.4319/lo.2011.56.2.0589, 2011.

Skidmore, R. E., Maberly, S. C., and Whitton, B. A.: Patterns of spatial and temporal variation in phytoplankton chlorophyll a in the River Trent and its tributaries, Science of the Total Environment, 210, 357–365, https://doi.org/10.1016/S0048-9697(98)00023-0, 1998.

Søballe, D. and Kimmel, B.: A large-scale comparison of factors influencing phytoplankton abundance in rivers, lakes, and impoundments, Ecology, 68, 1943–1954, https://doi.org/10.2307/1939885, 1987.

Sommer, U., Gliwicz, Z. M., Lampert, W., and Duncan, A.: The PEG-model of seasonal succession of planktonic events in fresh waters, Archiv für Hydrobiologie, 106, 433–471, 1986.

Sommer, U., Adrian, R., De Senerpont Domis, L., Elser, J. J., Gaedke, U., Ibelings, B., Jeppesen, E., Lürling, M., Molinero, J. C., Mooij, W. M., et al.: Beyond the Plankton Ecology Group (PEG) model: mechanisms driving plankton succession, Annual review of ecology, evolution, and systematics, 43, 429–448, https://doi.org/10.1146/annurev-ecolsys-110411-160251, 2012.

Wachholz, A., Jawitz, J. W., Büttner, O., Jomaa, S., Merz, R., Yang, S., and Borchardt, D.: Drivers of multi-decadal nitrate regime shifts in a large European catchment, Environmental Research Letters, 17, 064 039, https://doi.org/10.1088/1748-9326/ac6f6a, 2022.

Wachholz, A., Jawitz, J. W., and Borchardt, D.: From Iron Curtain to green belt: shift from heterotrophic to autotrophic nitrogen retention in the Elbe River over 35 years of passive restoration, Biogeosciences, 21, 3537–3550, https://doi.org/10.5194/bg-21-3537-2024, 2024.

Wagner, C. and Adrian, R.: Cyanobacteria dominance: quantifying the effects of climate change, Limnology and Oceanography, 54, 2460–2468, https://doi.org/10.4319/lo.2009.54.6_part_2.2460, 2009.

Wang, M., Bodirsky, B. L., Rijneveld, R., Beier, F., Bak, M. P., Batool, M., Droppers, B., Popp, A., van Vliet, M. T., and Strokal, M.: A triple increase in global river basins with water scarcity due to future pollution, Nature Communications, 15, 880, https://doi.org/10.1038/s41467-024-44947-3, 2024.

Weitere, M. and Arndt, H.: Top-down effects on pelagic heterotrophic nanoflagellates (HNF) in a large river (River Rhine): do losses to the benthos play a role?, Freshwater Biology, 47, 1437–1450, https://doi.org/10.1046/j.1365-2427.2002.00875.x, 2002.

Welker, M. and Walz, N.: Can mussels control the plankton in rivers?—a planktological approach applying a Lagrangian sampling strategy, Limnology and Oceanography, 43, 753–762, https://doi.org/https://doi.org/10.4319/lo.1998.43.5.0753, 1998.

Westphal, K., Graeber, D., Musolff, A., Fang, Y., Jawitz, J. W., and Borchardt, D.: Multi-decadal trajectories of phosphorus loading, export, and instream retention along a catchment gradient, Science of the Total Environment, 667, 769–779, https://doi.org/10.1016/j.scitotenv.2019.02.428, 2019.

Westphal, K., Musolff, A., Graeber, D., and Borchardt, D.: Controls of point and diffuse sources lowered riverine nutrient concentrations asynchronously, thereby warping molar N: P ratios, Environmental Research Letters, 15, 104 009, https://doi.org/10.1088/1748-9326/ab98b6, 2020.

https://doi.org/10.5194/egusphere-2026-830
Preprint. Discussion started: 28 April 2026

Whitehead, P. G., Wilby, R. L., Battarbee, R. W., Kernan, M., and Wade, A. J.: A review of the potential impacts of climate change on surface water quality, Hydrological sciences journal, 54, 101–123, https://doi.org/10.1623/hysj.54.1.101, 2009.

Wurtsbaugh, W. A., Paerl, H. W., and Dodds, W. K.: Nutrients, eutrophication and harmful algal blooms along the freshwater to marine continuum, Wiley Interdisciplinary Reviews: Water, 6, e1373, https://doi.org/10.1002/wat2.1373, 2019.

Yang, S., Büttner, O., Jawitz, J. W., Kumar, R., Rao, P. S. C., and Borchardt, D.: Spatial organization of human population and wastewater treatment plants in urbanized river basins, Water Resources Research, 55, 6138–6152, https://doi.org/10.1029/2018WR024614, 2019.